Applied Physics B (2025) 131:195
https://doi.org/10.1007/s00340-025-08564-2

Applied Physics B
Lasers and Optics

RESEARCH

Unravelling temporal dynamics in integrating cavities from nonuniform to uniform light fields

Zhiyang Sun[1,2] · Zhiguo Zhang[3] · Bin Yu[1] · Yongda Wang[5] · Lei Yang[2,4]

Received: 6 June 2025 / Accepted: 9 September 2025

Abstract

In this study, we investigate the light propagation characteristics within an integrating cavity, focusing on the transition from a non-uniform light field (NULF) to a uniform light field (ULF). We challenge the conventional assumption in integrating cavity theory that postulates the immediate establishment of a ULF upon light entry. Employing both experimental and simulation approaches, we derive the time constant of the integrating cavity under ULF conditions and measure the cavity's transient and steady-state responses. Our findings reveal that while a brief NULF phase precedes the ULF, the total radiant flux within the cavity adheres to the ULF propagation law from the onset. This study demonstrates that the NULF can be treated as an approximation of the ULF in terms of total radiant flux variation within an integrating cavity. Our study not only provides empirical validation for integrating cavity theories based on the ULF assumption but also presents compelling evidence of their efficacy in cavities with diverse geometries.

1 Introduction

An integrating cavity is fundamentally an enclosure whose inner surface is either made of or coated with a highly reflective, diffuse scattering material [1]. Serving as a versatile tool in optical laboratories, it excels in collecting and diffusing incident light, thereby facilitating a myriad of applications. These range from measuring the reflectance and transmittance of scattering materials [2, 3] to detecting weak absorption signals [4, 5], and acting as uniform light sources for imaging optics [6, 7]. Therefore, exploring the interaction mechanisms between light and integrating cavities is crucial for advancing the precision and efficacy of these devices, particularly in contexts where precise manipulation of light properties is crucial.

Current theories on integrating cavities are fundamentally based on the assumption that any point on the cavity's inner wall can be treated as an ideal Lambertian reflector [8–10]. This is crucial for the formation of a uniform light field (ULF) inside the cavity, characterized by the emission of light with equal intensity in all directions from any point within, following the first reflection of the incident light. This assumption has been validated through steady-state experiments and found to be applicable to various cavity shapes, including spheres, cubes, and cylinders [11–14]. However, recent research by Zhou et al. [15] revealed that, due to the actual inner wall of the cavity not being an ideal Lambertian scatterer, the light does not immediately form a ULF after the first reflection. Instead, a brief non-uniform light field (NULF) phase precedes the ULF. This NULF phase refers to the transient light field existing from the moment a light pulse is injected until the radiance becomes uniform at all points and from all directions within the cavity. The duration of this phase increases with the additional port fraction, a finding that challenges the ULF assumption pervasive in existing theories.

A clear understanding of the NULF is not merely of theoretical interest; it has significant practical implications, particularly in applications requiring high temporal resolution. For instance, when an integrating cavity is used for

✉ Lei Yang
yanglei@sensefuture.com

1 College of Physics and Optoelectronic Engineering, Shenzhen University, Shenzhen 518060, China

2 Shenzhen Institute for Technology Innovation, National Institute of Metrology, Shenzhen 518107, China

3 School of Instrument Science and Engineering, Harbin Institute of Technology, Harbin 150000, China

4 SenseFuture Technologies Co., Ltd, Shenzhen 518107, China

5 Yongkang Hardware College, Zhejiang University of Technology, Yongkang 321300, China

Published online: 24 September 2025

time-resolved spectroscopy, fluorescence lifetime measurements, or the impulse response characterization of high-speed photodetectors, the initial portion of the measured output signal is inherently dominated by the NULF. Without a proper physical model, researchers might misinterpret this complex initial signal—with its fast rise and varying shape—as an artifact or a feature of the system under test, leading to inaccurate conclusions.

In this study, we delve into the genesis of the NULF and its possible impact on the integrating cavity theory based on the ULF assumption. We derive the time constant of the cavity under ULF conditions and measure both the steady-state and transient responses of the cavity. Through comparative analysis of the effective optical path length (EOPL), we identify the appropriate methodology for calculating the time constant. Finally, we simulate the light propagation process within the integrating cavity, extracting the total radiant flux as a function of time based on the simulation results.

2 Theory

The transition from a NULF to a ULF within an integrating cavity fundamentally refers to the gradual shift from an uneven to an even spatial distribution of the light field over time. To investigate the nature of the NULF and its potential impact on the cavity theory based on a ULF, we first derive the time constant of the integrating cavity under ULF conditions. It is posited that when light enters through the cavity's entrance aperture, a ULF is established following N reflections. We designate the moment the ULF forms in the cavity as $t = 0$, with the radiant flux in the cavity being Φ at this instant. During the time span $t = 0$ to τ, the light undergoes an average of R reflections inside the cavity. Here, τ is the time constant of the cavity and can be expressed as [16]:

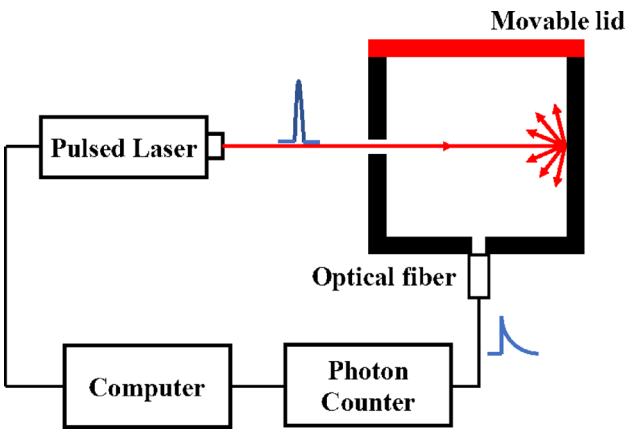

Fig. 1 Schematic of the experimental setup for temporal response measurements of a cubic cavity

$$\tau = R\bar{t} = R\frac{L_{ave}}{c} \tag{1}$$

where $\bar{t}$ is the average time between successive reflections, L_{ave} is the single-pass average path length, equal to $4V/S$, with V representing the volume and S the inner surface area of the cavity. c is the speed of light. To ascertain R in Eq. (1), we look at how the remaining radiant flux in the cavity varies with time. After the ULF is formed in the cavity, at the first reflection, the radiant flux in the cavity becomes $[\rho(1-f)]\Phi$. ρ is the diffuse reflectance of the cavity wall, and f is the total port fraction. After R reflections, the radiant flux remaining in the cavity is $[\rho(1-f)]^R\Phi$. By definition, the time constant τ is the time required for the radiant flux to decrease to Φ/e. For a highly reflective integrating cavity with small apertures, the approximations $f \approx 0$ and $\rho \approx 1$ are reasonable. Under these conditions, the time constant can be derived as [17–19]:

$$\tau = \frac{\rho}{1-\rho(1-f)}\frac{L_{ave}}{c} = M\frac{L_{ave}}{c} = \frac{L_{eff}}{c}, \tag{2}$$

where L_{eff} denotes the EOPL of the cavity. To interpret Eq. (2) in terms of EOPL, we can rewrite it as:

$$L_{eff} = \tau c. \tag{3}$$

According to Eq. (3), the EOPL can be determined by multiplying the time constant by the speed of light. However, this formula is strictly applicable only when the cavity manifests as a ULF and does not account for the effects of NULF, that is, the initial N reflections leading to the formation of the ULF. If NULF effects are included, the calculated time constant could differ. To ascertain whether the influence of NULF should be considered in calculating the time constant, we conducted experiments to measure both the transient and steady-state response of the integrating cavity, as elaborated in the following sections.

3 Experiments

A schematic of the experimental setup used for temporal response measurements of an integrating cavity is illustrated in Fig. 1. An integrating cube with a side length of 8 cm was employed. The inner surface of the cavity was coated with a barium sulfate-based coating Avian-D [20] supplied by Avian Technologies. A specially designed movable lid was implemented to generate a continuously adjustable additional port fraction. A 405 nm picosecond pulsed laser (NKT Photonics-Superk Extreme) with a FWHM of 0.7 ns was utilized as the light source. The output pulse was

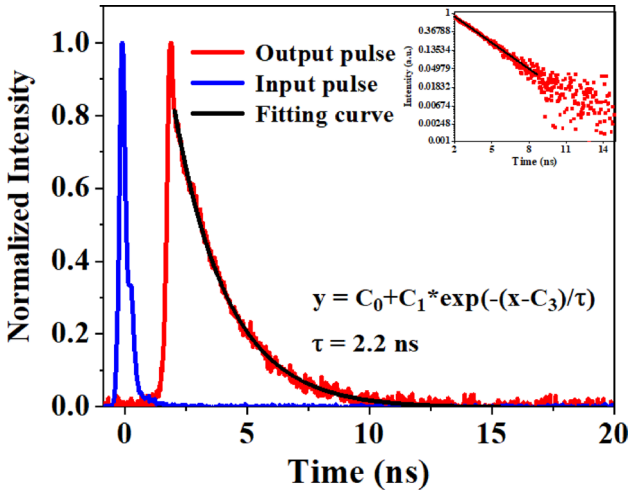

Fig. 2 Temporal response curve of a cubic cavity for $f = f_0$

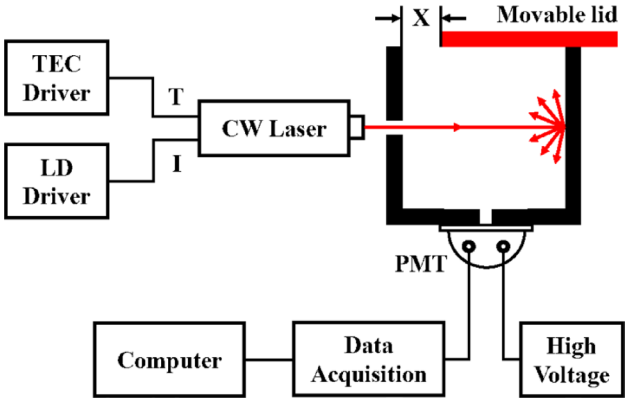

Fig. 3 Schematic of the experimental setup for measuring the steady-state response of a cubic cavity

captured by a photon counter (Becker and Hickl GmbH, PMC-100-1). Throughout the temporal response measurement, the movable lid remained closed, signifying that $f = f_0$. Here, f_0 is the initial port fraction, defined as the sum of all the initial port areas divided by the total internal surface area of the cavity.

Typically, the intensity of the output pulse is significantly lower than that of the input pulse. However, as the absolute value of the pulse is not crucial to this study, both the input and output pulses are normalized to facilitate comparison, as illustrated in Fig. 2. Analysis of the integrating cavity's output pulse curve provides a direct method for identifying the NULF and quantifying its duration. The principle is that the NULF phase precedes the establishment of the ULF, the latter of which is characterized by a pure exponential decay. Therefore, by fitting an exponential function to the decaying tail of the measured pulse, as shown in Fig. 2, we can identify the onset of the ULF phase. The entire time interval before this point, from the initial light injection until the start of the exponential decay, is consequently defined as the NULF. The inset demonstrates the results on a natural logarithm (ln) ordinate, revealing a linear decay of the output radiant flux. Notably, after the input pulse enters the cavity, it takes some time for a ULF exhibiting exponential decay to establish itself. In this initial phase, the light field inside the cavity remains non-uniform. Regarding the trailing edge of the output pulse, which aligns with the ULF, τ is determined either by fitting the trailing edge of the output pulse or by employing the subsequent formula:

$$\tau = \frac{\int_0^\infty tI(t)dt}{\int_0^\infty I(t)dt}, \tag{4}$$

Here, $I(t)$ denotes the cavity's emitted light intensity, where I is a function of time t. Considering only a ULF, Eq. (3) yields $\tau = 2.2(1)$ ns and $L_{eff} = 66(3)$ cm. However, incorporating the NULF in the cavity as per Eq. (4), we obtain $\tau = 3.7(1)$ ns and $L_{eff} = 111(3)$ cm. This indicates a notable difference when employing these two methods. To ascertain which method is accurate, we employed an alternative, validated method proposed by Sun to calculate the EOPL of the integrating cavity. This technique involves measuring the cavity's steady-state response under varied port fractions. The EOPL is determined using the following relationship [21]:

$$L_{eff} = L_0 + \frac{L_{ave}}{1/\rho - (1 - f_0)}. \tag{5}$$

Here, L_0 is additional path length which depends on the specific launch and delaunch conditions [22]. According to Eq. (5), determining L_{eff} requires knowledge of all the four quantities on the right side of Eq. (5). Therefore, the approach begins with measuring the cavity's output radiant flux under various conditions of additional port fraction. These measurements are then subjected to curve fitting to derive the values of f_0 and ρ. Subsequently, by inputting the additional path length L_0 and the single-pass average path length L_{ave} into Eq. (5), we can compute L_{eff}. The experimental setup and the resulting measurements are presented in Figs. 3 and 4.

Figure 3 illustrates the experimental arrangement for measuring the steady-state response of a cubic cavity. Due to the variation in the EOPL of the integrating cavity with wavelength, a laser diode (Nichia, NDHV210, 120mW) with a wavelength of 405 nm was employed as the light source in steady-state experiments to determine the EOPL of the cavity at 405 nm. To maintain a consistent laser output, we mounted the diode on a thermoelectrically-cooled base (Thorlabs, TCLDM9). We regulated the temperature and current of the laser diode using a temperature controller (Thorlabs, TED 200C, −45 °C to +145 °C, ±0.01 °C)

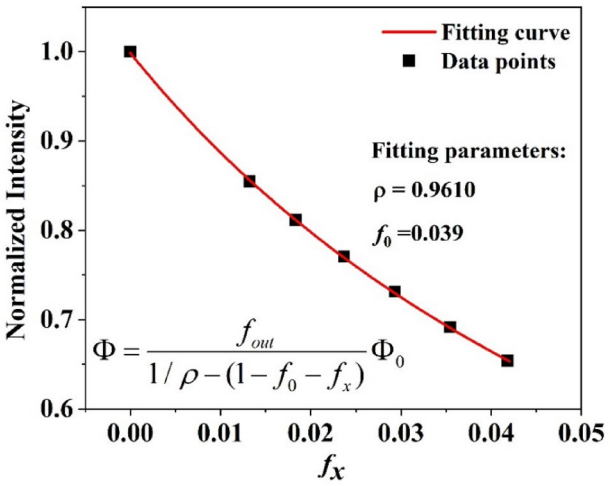

Fig. 4 Steady-state response of a cubic cavity when $f = f_0 + f_x$

and a current controller (Thorlabs, LDC 205C, 0–500 mA, ±0.1 mA), respectively. The emitted light was captured by a PMT (Zolix Instruments, CR131) and transformed into a digital signal through a data acquisition system (Zolix Instruments, DCS103). During experiments, we introduced an adjustable additional port fraction f_x by manipulating the movable lid of the cavity, as depicted in Fig. 3. We then recorded the output radiant flux at various f_x values, with the measurement results presented in Fig. 4.

As demonstrated in Fig. 4, the cavity's output radiant flux is observed to decrease with an increase in the additional port fraction, f_x. This reduction is attributed to the escape of more light through the added aperture as f_x increases, leading to a weakened internal light field within the cavity and consequently diminishing the light intensity detected by the sensor [23]. By employing the formula in Fig. 4 to fit the data points, we determined the values of the fitting parameters ρ and f_0 to be 0.9610 and 0.039, respectively. Considering the additional path length L_0 and the single-pass average path length L_{ave}, the EOPL of the cavity is calculated to be 67.0(8) cm. This value is in close agreement with the EOPL derived solely from ULF considerations, validating the use of ULF for calculating the time constant based on the cavity's temporal response. A discrepancy of 1 cm in the EOPL values obtained from time-resolved spectroscopy and the method proposed by Sun is observed. This discrepancy is primarily attributable to two sources of error: uncertainties in the cavity dimensions and in the time constant measurement. Dimensional inaccuracies in the cavity, affecting L_{ave}, arise due to variability in cutting and assembly processes of the cavity, contributing to an estimated 1 mm uncertainty in the cavity's side length. This leads to a relative uncertainty of 1.25% in L_{eff}, as per Eq. (3) and basic error propagation principles. The uncertainty in the time constant, determined from standard error values of the exponential fit in Fig. 2, is 0.12 ns. According to Eq. (3) and basic error propagation, this results in a relative uncertainty of 5.5% in L_{eff} due to the time constant.

4 Results and discussion

Our analysis begins with the experimental results shown in Fig. 2, which provide direct evidence for the anisotropic nature of the NULF. The fundamental principle of an integrating cavity is that a fully established ULF is, by definition, isotropic. This means its decay, observed from any direction, must follow a pure exponential law, which is represented by the black fitting curve in our analysis. Our experimental measurement, however, is inherently directional, capturing the flux from a single port. The measured signal (the red curve) clearly deviates from the ideal isotropic model during its initial phase. This deviation is the definitive experimental proof of the NULF's anisotropy. It is not a potential effect, but a direct observation. The origin of this anisotropy is the physical process of the light field's evolution, and its quantification is captured by the shape and magnitude of this difference between our directional measurement and the theoretical isotropic decay.

The anisotropy observed in our experiment raises a fundamental question: does the total radiant flux, integrated over the entire cavity, still follow a simple exponential decay even during the NULF phase? A direct experimental answer is challenging, as any single detector provides only a directional view. To overcome this limitation and directly investigate this central question, we leveraged finite element analysis using COMSOL Multiphysics. This simulation was designed not merely to model the process, but to calculate the true total radiant flux, independent of direction. We modeled a cubic integrating cavity with a 12 cm side length. Upon the first reflection of the incident light off the cavity walls, 100,000 diffuse rays in various directions were generated, simulating multiple diffuse reflections within the cavity. Rays impacting the input and output apertures ceased to reflect, their energy thus excluded from the cavity's total radiant flux. The simulation continued until the total radiant flux decayed to a predetermined level. MATLAB was utilized to process the raw simulation data, producing a time-dependent curve of the cavity's total radiant flux, as shown in Fig. 5.

The simulation results presented in Fig. 5 are unequivocal. They demonstrate a near-perfect exponential decay of the total energy from the moment of light injection ($R^2 = 0.9998$). This finding provides the definitive answer to our question. By comparing the complex, directional signal from our experiment (Fig. 2) with the simple, total flux signal from our simulation (Fig. 5), we can now decisively

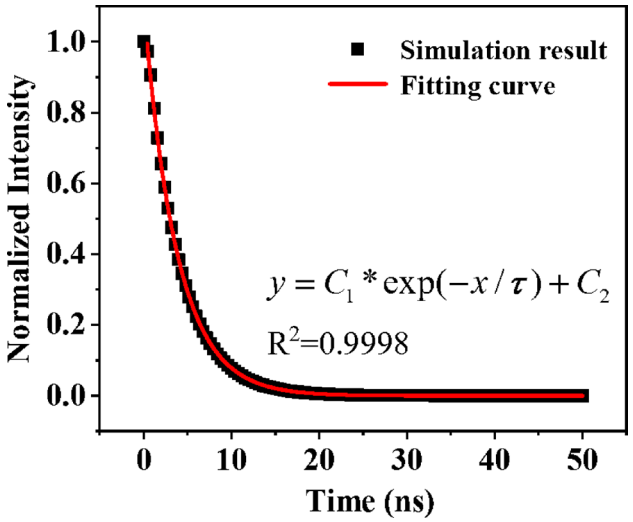

Fig. 5 Simulation of the total radiant flux in the integrating cavity with time

conclude that the intricate shape of the measured pulse is not a failure of the exponential decay law for the cavity's total energy. Instead, it is purely a consequence of making a directional measurement while the light field is still in its anisotropic, non-uniform phase. This insight is crucial: it elucidates that the rising edge of a measured pulse does not represent the behavior of the total flux, but rather signifies changes in the flux along a specific observational direction, attributable to the anisotropy of the NULF. This validates treating the light field as a ULF from the moment of light entry for calculations based on total energy, such as the time constant, providing robust support for existing integrating theories [8, 10].

It is important to note that the NULF is a real phenomenon that always precedes the formation of a ULF inside the cavity. For the specific task of calculating the cavity's time constant, our experiments demonstrate that disregarding the NULF phase still yields an accurate result. However, this specific finding should not be generalized to mean that the influence of the NULF is always negligible. The impact of the NULF becomes significant in other scenarios. For instance, in cases involving cavities that are very large, possess highly irregular shapes, or whose inner walls cannot be approximated as ideal Lambertian surfaces (e.g., those with a specular reflection component), the light field typically requires a longer time to homogenize. Consequently, the duration of the NULF would be longer, and its effect on measurements would be much more pronounced.

Further, this study broadens our understanding of integrating cavities with different shapes. While a spherical cavity ideally aligns with the ULF assumption, as per the theory of radiation exchange within diffuse surface enclosures, other shapes like cubic or cylindrical cavities, though approximations, are still effectively described by ULF-based theories. This insight paves the way for a more universally applicable theory of integrating cavities, based on the assumption of a ULF.

5 Conclusions

In summary, our research on integrating cavities provides a refined understanding of the light propagation process within these optical components. The primary discovery of a transient NULF phase that precedes the establishment of a ULF adds depth to the existing theory of integrating cavities. Despite the initial non-uniformity, the overall radiant flux decay within the cavity conforms to the ULF propagation law, suggesting that the impact of NULF on the time constant calculations is negligible. This insight aligns with our experimental observations and is further corroborated by simulation results. Consequently, integrating cavity theories, especially those assuming a ULF, remain robust and applicable even in the presence of an initial NULF. The findings from this study have significant implications for the design and application of integrating cavities in optical measurements, broadening the potential for their use in specialized areas such as diffuse reflectance spectroscopy and photometric calibration, where nuanced control of light behavior is essential.

Acknowledgements This work was supported by the Guangdong Basic and Applied Basic Research Foundation (2019A1515111199) and the Special Fund Project of Shenzhen Municipal Market Supervision Administration: Research on Foreign Technical Trade Measures and Technologies for Integrated Circuit Precision Testing Equipment (242000023002149).

Author contributions Zhiyang Sun: Conceptualization, Methodology, Validation, Formal analysis, Investigation, Resources, Data curation, Writing- Original draft preparation. Bin Yu and Yongda Wang: Validation, Data curation. Lei Yang and Zhiguo Zhang: Conceptualization, Methodology, Supervision.

Data availability Data underlying the results presented in this paper are not publicly available at this time but may be obtained from the authors upon reasonable request.

Declarations

Conflict of interest The authors declare no competing interests.

References

1. X. Zhou, J. Yu, L. Wang, Z. Zhang, Investigating the relation between absorption and gas concentration in gas detection using a diffuse integrating cavity. Appl. Sci. **8**(9), 1630 (2018)

2. Q. Gao, J. Yu, Y. Zhang, Z. Zhang, W. Cao, Diffuse reflectance measurement using gas absorption spectroscopy. Sens. Actuators B Chem. **196**, 147–150 (2014)
3. H. Shitomi, I. Saito, A new absolute diffuse reflectance measurement in the near-IR region based on the modified double-sphere method. Metrologia **46**(4), S186 (2009)
4. X. Zhou, J. Yu, L. Wang, Q. Gao, Z. Zhang, Sensitive detection of oxygen using a diffused integrating cavity as a gas absorption cell. Sens. Actuators B Chem. **241**, 1076–1081 (2017)
5. T. Jávorfi, J. Erostyák, J. Gál, A. Buzády, L. Menczel, G. Garab, K.R. Naqvi, Quantitative spectrophotometry using integrating cavities. J. Photochem. Photobiol. B Biol. **82**(2), 127–131 (2006)
6. M. Vacula, P. Horvath, L. Chytka, K. Daumiller, R. Engel, M. Hrabovsky, D. Mandat, H.-J. Mathes, S. Michal, M. Palatka et al., Use of a general purpose integrating sphere as a low intensity near-UV extended uniform light source. Optik **242**, 167169 (2021)
7. Labsphere, Integrating sphere uniform source applications. (n.d.), Retrieved from https://www.labsphere.com/wp-content/uploads/2021/09/Integrating-Sphere-Uniform-Source-Applications.pdf
8. Labsphere, Integrating sphere theory and applications. (n.d.), Retrieved from https://www.labsphere.com/wp-content/uploads/2021/09/Integrating-Sphere-Theory-and-Applications.pdf
9. Labsphere, Integrating sphere radiometry and photometry. (n.d.), Retrieved from https://www.labsphere.com/wp-content/uploads/2021/09/Integrating-Sphere-Radiometry-and-Photometry.pdf
10. SphereOptics, Integrating sphere design and applications. (n.d.), Retrieved from http://www.sphereoptics.com/assets/sphere-optic-pdf/sphere-technical-guide.pdf
11. G. Feng, Y. Wang, Y. Ma, P. Li, C. Zheng, A non-standard auxiliary integrating sphere and correction method for the realization of diffuse reflectance. Optik **124**(20), 4325–4327 (2013)
12. L. Wang, Measuring optical absorption coefficient of pure water in UV using the integrating cavity absorption meter. Texas A&M University. Note: This appears to be a dissertation/thesis, formatted as a book (2008)
13. P. Elterman, Integrating cavity spectroscopy. Appl. Opt. **9**(9), 2140–2142 (1970)
14. M.T. Cone, J.A. Musser, E. Figueroa, J.D. Mason, E.S. Fry, Diffuse reflecting material for integrating cavity spectroscopy, including ring-down spectroscopy. Appl. Opt. **54**(2), 334–346 (2015)
15. X. Zhou, J. Yu, L. Wang, Z. Zhang, Measurement of the effective optical path length of diffusing integrating cavities using time-resolved spectroscopy. Appl. Opt. **57**(13), 3519–3523 (2018)
16. E.S. Fry, J. Musser, G.W. Kattawar, P.-W. Zhai, Integrating cavities: temporal response. Appl. Opt. **45**(36), 9053–9065 (2006)
17. Q. Gao, Y. Zhang, J. Yu, Z. Zhang, S. Wu, W. Guo, Integrating sphere effective optical path length calibration by gas absorption spectroscopy. Appl. Phys. B **114**(3), 341–346 (2014)
18. J. Yu, F. Zheng, Q. Gao, Y. Li, Y. Zhang, Z. Zhang, S. Wu, Effective optical path length investigation for cubic diffuse cavity as gas absorption cell. Appl. Phys. B **116**(1), 135–140 (2014)
19. J. Yu, Q. Gao, Z. Zhang, High reflected cubic cavity as long path absorption cell for infrared gas sensing. in *Infrared Sensors, Devices, and Applications IV*, Vol 9220 (SPIE, 2014), pp. 150–161.
20. Avian Technologies (n.d.). Avian-D White reflectance coating. Retrieved 1 May 2022, from https://aviantechnologies.com/product/avian-d-white-reflectance-coating/
21. Z. Sun, Y. Wang, R. Zhang, Z. Zhang, Determination of the effective optical path length of integrating cavity by measuring emitted light. Appl. Phys. B **130**(1), 9 (2024)
22. J. Hodgkinson, D. Masiyano, R.P. Tatam, Using integrating spheres as absorption cells: path-length distribution and application of Beer's law. Appl. Opt. **48**(30), 5748–5758 (2009)
23. Z. Sun, Y. Wang, Z. Zhang, Effect of port fraction on the radiant flux of the integrating cavity. Appl. Phys. B **129**(6), 102 (2023)